JOURNAL OF GEOPHYSICAL RESEARCH, VOL. 89, NO. A5, PAGES 2823–2830, MAY 1, 1984

Direct Multiple Path Magnetospheric Propagation: A Fundamental Property of Nonducted VLF Waves

VIKAS S. SONWALKAR, T.F.BELL, R.A.HELLIWELL, U.S.INAN

Space, Telecommunications and Radioscience Laboratory, Stanford University

ISEE 1 satellite observations of nonducted whistler mode signals from the Siple Station VLF transmitter show that all well-defined pulses (S/N $\approx$ 20 dB) are elongated by 20 ms to 200 ms. This elongation is attributed to closely spaced multiple paths of propagation between the ground and the satellite. The presence of multiple paths is further confirmed by the observed amplitude fading pattern where fading occurs not only at half the spin period (1.52 s) of the rotating antenna but also at time scales of the order of 1 s. Electric field measurements show a 2 to 10-dB amplitude variation, which is again consistent with direct multiple path propagation. We illustrate the results with two cases : one on October 29, 1977, inside the plasmapause and the other on May 7, 1979, outside the plasmapause. Our results establish that, in general, at any point in the magnetosphere the direct signals transmitted from the ground arrive almost simultaneously along two or more closely spaced direct ray paths. It is shown that multiple paths can be explained by assuming field-aligned irregularities of 1 to 10-km horizontal scale in the ionosphere with a few percent enhancement or depletion in the plasma density. We discuss the implications of our results for nonducted wave-particle interaction in the earth's magnetosphere. We show that for reasonable parameters of nonducted multiple path propagation, a cyclotron resonant electron will experience a wave doppler broadening of a few tens of hertz to a few hundreds of hertz.

1. INTRODUCTION

ISEE 1 satellite observations of nonducted whistler mode waves from the Siple station VLF transmitter reveal a new phenomenon involving direct multiple path propagation. Our results establish that, in general, at any point in the magnetosphere the direct signals transmitted from the ground arrive almost simultaneously along two or more closely spaced direct ray paths. A typical experimental configuration during our observations is shown in Figure 1*a*. The electric field data were analyzed for roughly 100 orbits during a 2-year period, from October 1977 to December 1979. The frequency of occurence of Siple signal reception was 25 %. On 12 passes the Siple signal was observed for more than 10 to 15 min continuously with a S/N = 20 dB (in a 300-Hz band), and these observations form the data base for the present study.

Our observations are detailed in section 3 and are summarized as follows:

1. All measurable pulses (S/N = 20 dB when measured with a 300-Hz bandwidth filter) show elongations varying from 20 ms to 200 ms (section 3.1).

2. High spatial resolution peak electric field measurements show 2 to 10-dB amplitude variation (section 3.2).

3. Observed amplitude fading occurs not only at half the spin period (1.5 s) of the rotating antenna but also at time scales of the order of 1 s (section 5).

These observations are attributed to closely spaced multiple propagation paths (see rays 1 and 2 as shown in Figure 1*a*) between the ground and the satellite (section 4).

The importance of our result lies in the fact that the multiple path propagation is very common and has significant effects on the physics of wave-particle interactions and cold plasma diagnostics in the magnetosphere (section 6).

Copyright 1984 by the American Geophysical Union.

Paper number 4A0157.
0148-0227/84/004A-0157$05.00

Nonducted waves may propagate in the magnetosphere with any wave normal direction which lies within the resonance cone. When magnetospheric waves reach the ionosphere their wave normals usually lie outside the transmission cone and hence are not observed on the ground, but in general these waves can be observed on a satellite [*Helliwell,* 1965]. In the direct nonducted mode, a ray travels from the ground to the satellite with no reflection (in the magnetosphere) in between. In the case of a magnetospherically reflected mode, a VLF signal transmitted from the ground propagates along a ray path which undergoes one or more reflections in the magnetosphere before reaching the satellite (Figure 1*b*). This mode has been studied in the past and does not concern us here [*Walter,* 1969; *Edgar,* 1973]. There is another mode of propagation called ducted propagation in which the VLF energy travels inside ducts of enhanced or depleted ionization with wave normal closely aligned with the geomagnetic field (Figure 1*b*). When ducted signals reach the ionosphere, their wave normals usually lie within the transmission cone and therefore can be observed on the ground (e. g., a natural whistler). A signal transmitted from the ground can propagate through more than one duct (in the presence of such ducts) and be observed on the ground. This is called ducted multiple path propagation [*Smith et al.,* 1960]. In this paper we consider only the direct nonducted mode of propagation from the Siple Station transmitter to the ISEE 1 satellite. We show that at any point in the magnetosphere signals arrive from the ground almost simultaneously (within 20 ms to 200 ms) along two or more direct nonducted ray paths. We call this mode of propagation direct multiple path propagation. We provide an interpretation of the phenomenon by assuming the presence of 1 to 10-km horizontal scale irregularities of a few percent enhanced/depleted ionization in the ionosphere. We shall also indicate the applications and implications of our findings to cold plasma diagnostics and nonducted VLF wave particle interactions.

In the past, *Heyborne* [1966] and *Scarabucci* [1969] have observed amplitude fading on the low altitude ($\approx$ 1000 km)

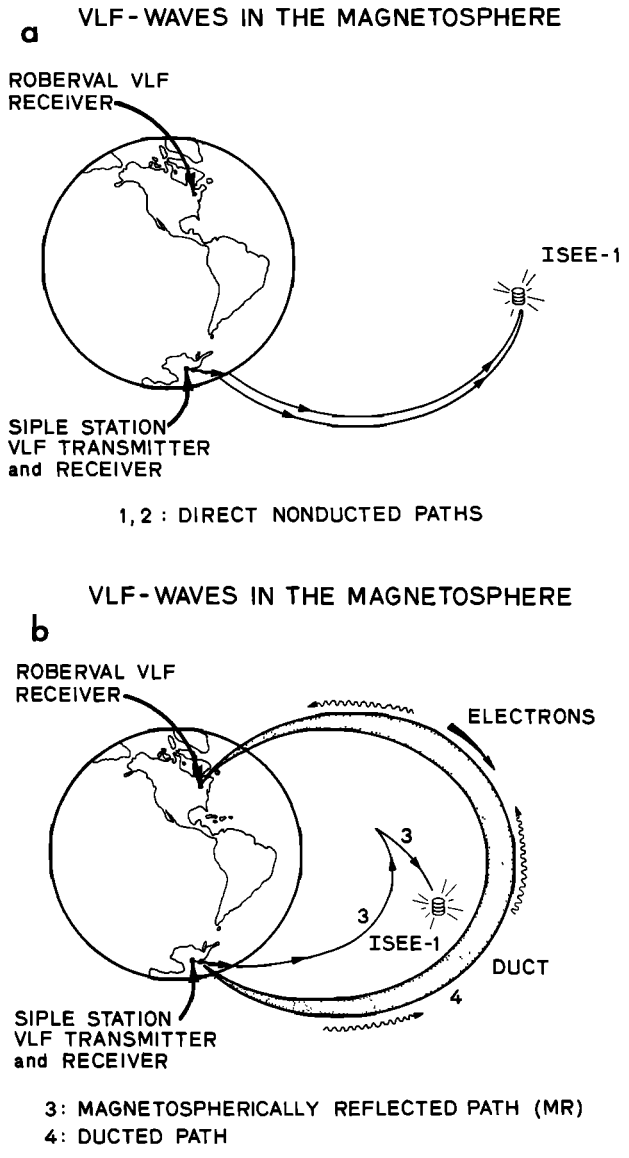

Fig 1. Schematic representation of the Stanford University VLF wave injection experiment on the ISEE-1 satellite. (*a*) Siple to ISEE 1 transmission by two direct nonducted ray paths that start at different latitudes at 500 km and arrive almost simulteneously at the ISEE 1 satellite (rays 1 and 2). (*b*) Siple to ISEE 1 transmission by a magnetospherically reflected path (ray 3), and Siple to Roberval transmission through a field-aligned duct of enhanced ionization (ray 4).

OGO 1, OGO 2, and OGO 4 satellites. Also *Cerisier* [1973] has observed two doppler shifts in the FUB transmitter signal observed on the FR 1 satellite (altitude $\approx$ 750 km). These authors have interpreted their observations as indicating the presence of two waves. More recently, pulse elongations and amplitude modulations have also been observed in Omega pulses received on the GEOS satellite [*Neubert et al.*, 1983] and these measurements are consistent with our observations. Our work relates to observation of multiple paths in the high altitude ($\approx$ 25,000 km) magnetosphere and over a wide range of L shells (L=2.8 to 11.5). We show evidence both by high resolution time delay analysis as well as theoretical analysis of fading patterns that multiple path propagation is a common phenomenon in the magnetosphere. Previous work is consistent with the general picture of multiple path propagation that we have developed here.

Our study is a part of Stanford University's wave injection experiment [*Bell and Helliwell*, 1978] involving the ISEE 1 spacecraft, the VLF transmitter at Siple Station, Antartica, and a VLF receiving site at Roberval, Canada. It is aimed at a better understanding of VLF wave particle interaction in the earth's magnetosphere. Preliminary observations of Siple signal and associated triggered emissions on the ISEE 1 satellite were reported by Bell and others [*Bell et al.*, 1981, 1983]. The phenomenon we describe in this paper was first reported at the 1982 fall conference of American Geophysical Union in San Francisco [*Sonwalkar et al.*, 1982].

2. Experiment Background

The experiment is based on the observations of Siple signals by the ISEE 1 satellite. It has four main components: (1) A broadband (1 to 32 kHz) VLF receiver on ISEE 1 connected to a 215-m long electric antenna, (2) a broadband (1 to 20 kHz) VLF transmitter located at Siple Station, Antarctica [*Helliwell and Katsufrakis*, 1974], (3) various VLF navigation and communication transmitters, such as those of worldwide Omega Network, and (4) ground stations in the Antartic and Canada. During the ISEE 1 wave injection experiments from Siple Station several transmission formats were used. They included fixed frequency pulses of variable duration and frequency ramps of both positive and negative slopes. Each format is designed to investigate one or more specific questions concerning the physics of wave particle interactions in the magnetosphere. In this paper we concentrate on fixed frequency pulses of 0.5-s to 20.0-s duration. The pulse frequency ranges from 3.5 kHz to 5.5 kHz.

3. Observations

Data were analyzed over a 2-year period, from October 1977 to December 1979 and will be illustrated by considering two cases in detail :

1. May 7, 1979 : Siple signals were received con-

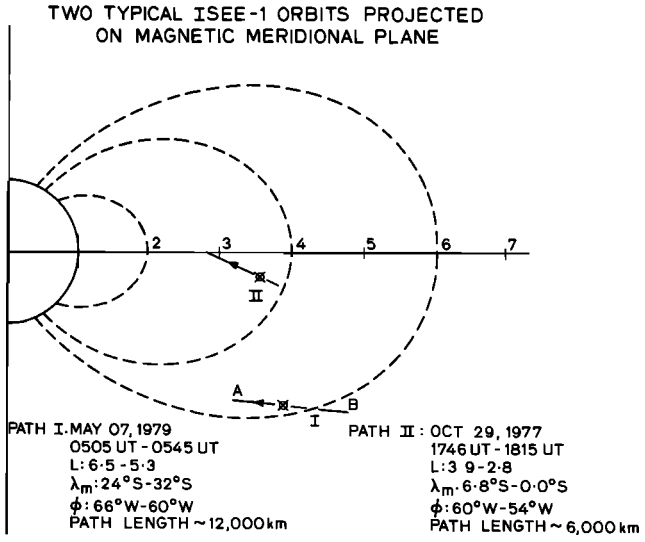

Fig 2. Two typical ISEE 1 orbits projected on the Siple-Roberval magnetic meridional plane. Case 1, May 7, 1979, ISEE 1 received Siple signals continuously over a path length of 12,000 km outside the plasmapause; case 2, October 29, 1977, ISEE 1 received signals continuously over a path length of 6,000 km inside the plasmapause. These days are analyzed in detail for illustration.

tinuously between 0505 UT and 0545 UT over a satellite trajectory of length 12,000 km, outside the plasmapause.

2. October 29, 1977 : Siple signals were received continuously between 1746 UT and 1815 UT over a satellite trajectory of length 6,000 km, inside the plasmapause.

Figure 2 depicts these trajectories when projected on the Siple - Roberval magnetic meridional plane.

Figure 3 shows samples of data received on ISEE 1 on the two days in question. The top panel shows the spectrogram of a Siple signal received on ISEE 1 for the October 29, 1977, case. The part of the satellite trajectory over which the signal was received is shown in Figure 2. Another spectrogram with higher time resolution (20 ms) was used to measure time delays. On the average, 1 s long pulses were transmitted every 4 s giving a spatial resolution of 20 km. The pulse frequency was 6.0 kHz. The particular example shown here depicts the part of the format when pulses of length varying from 50 ms to 200 ms were transmitted. Spatial resolution for this example varies from 200 m to 1 km.

The second panel shows the amplitude of the electric field component in the spin plane of the antenna observed with a 300-Hz bandwidth filter centered at 6.0 kHz. Amplitude charts of this kind were used to measure time delays, field intensities, and to perform a wave normal analysis (described later).

The third panel shows the spectrogram of the Siple signal received on ISEE 1 for the May 7, 1979, case. The part of the trajectory where the signal was observed on this day is shown in Figure 2. Pulses of 0.5 s to 20 s length were transmitted at 4.0 kHz for the first 20-min period (0505 to 0545 UT), and at 5.5 kHz for the next 20 min period (0525 to 0545 UT). Pulses were transmitted 6 to 12 times per minute, giving a spatial resolution of 25 km to 50 km (satellite speed $\approx$ 5 km/s).

The fourth panel shows the amplitude of the electric field component in the spin plane of the antenna for the spectrogram shown in panel 3. The signal was processed with a 300-Hz bandwidth filter centered at 4.0 kHz The observed amplitude fading patterns are complicated and noteworthy. The fading period of approximately 1.5 s results from the regular 3.0-s spin period of the satellite. Other periods (of the order of 1 s) are introduced because of the presence of multiple paths as explained in section 4.

3.1. *Time Delays*

Time delays associated with a pulse were measured with 20-ms accuracy both from spectrograms and amplitude charts. When a pulse reaches the satellite by more than one path, there are different time delays associated with each path. The method employed here can in general measure only the shortest and the longest time, which are defined as follows :

First Time Delay, T_f : If the leading edge of a T second long pulse was transmitted from the ground at time t, and the leading edge was received at time "t_f", then,

$$T_f = t_f - t$$

Last Time Delay, T_l : If the leading edge of a T second long pulse was transmitted at time t, and its trailing edge was received at time "t_l", then

$$T_l = t_l - (t + T)$$

Both the leading and the trailing edges were defined as the time when the pulse amplitude was 10 dB below the peak pulse amplitude.

Pulse Elongation, ΔT :

$$\Delta T = (t_l - t_f) - T = T_l - T_f$$

The definitions outline the procedure for making time delay measurements. Both T_f and T_l were measured for each pulse transmitted from the Siple Station transmitter and received on ISEE 1. About 5 to 10 pulses of typically 1 to 20 s duration were transmitted every minute and received on the satellite for a period of 25 min on October 29, 1977, and for a period of 40 min on May 7, 1979. More than 90 % of the pulses from which the time delay data were obtained were received on the satellite with a signal to noise ratio of more than 20 dB.

Figures 4*a* and 4*b* show typical time delay measurements for a 5-min interval of the May 7, 1979, case and of the October 29, 1977, case, respectively. Similar time delays were seen on other days of Siple signal reception on the ISEE 1 satellite. The squares and crosses represent T_f and T_l, respectively. The bars joining corresponding squares and crosses give the pulse elongations of the respective pulses. The dots in these figures give electric field amplitude data explained later. Here we introduce a few more definitions for convenience. One is the T_f curve which is the locus of T_f along the satellite trajectory. Another is the T_l curve which is the locus of T_l along the satellite trajectory.

From the time delay data we observe the following general features of nonducted wave propagation in the magnetosphere.

1. The T_f curve is relatively smooth.
2. Almost all pulses show elongation. (At some places in Figures 4a and 4b, T_l measurements are missing. This is because the trailing edge of those pulses was buried in noise.)
3. Pulse elogations vary rapidly from 20 ms to 200 ms in a relatively short period of 5 to 10 s. On the average compared to the T_f curve, the T_l curve is not smooth.
4. On the average the pulse elongation is independent of the pulse length T itself.

Some elaboration is required regarding the relatively smooth nature of the T_f curve. What is meant here is that in general over an interval of 30 to 60 s the first time delay, T_f, will show a rather smooth variation ($\approx$ 20 ms) from pulse to pulse; whereas over the same time interval the last time delay, T_l, generally varies from 20 to 200 ms. This observation is based in the average sense on long satellite trajectories of length $\approx$ 10,000 km. Sometimes the first time delay shows rapid variations (e.g., the last half minute period in Figure 4*a*).

There is another kind of pulse elongation not considered here, associated with triggered nonducted VLF emissions [*Bell et al.*,1981]. Its distinguishing features are a bandwidth increase and large changes in the electric field intensity.

A VLF pulse undergoes distortion as it travels through the dispersive magnetosphere[*Chang,* 1978]. This distortion is important for short pulses ($\approx$ 10 ms long). In our case, 1 s long pulses at 5 kHz have a bandwidth of the order of 1 Hz, and the pulse distortion is estimated to be $\approx$ 1 ms, a value much less than our measurement error of 10 ms.

The fact that almost all the pulses are elongated and that the pulse elogations are independent of pulse length is

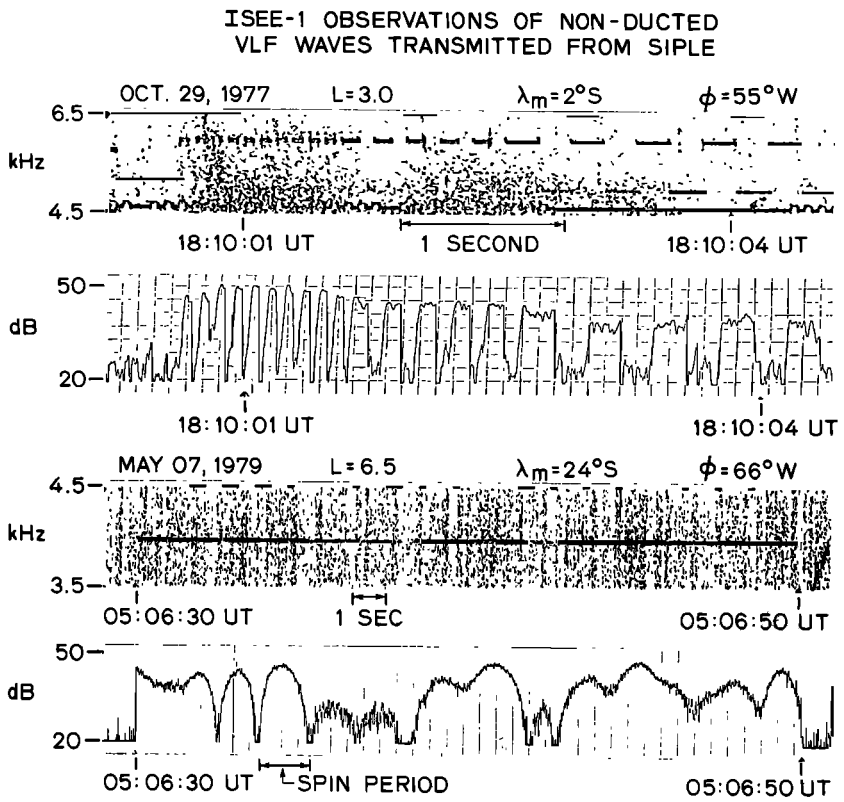

Fig 3. Two examples of the data received on ISEE 1 satellite for the two passes shown in Figure 2. The top two panels show the spectrogram and electric field intensity (100-Hz filter) for a variable pulse length format received on October 29, 1977. The bottom two panels give a similar data for a 20-s long pulse received on ISEE 1 on May 7, 1979.

clear evidence of the omnipresence of multiple paths. The magnitudes of pulse elongations, and the ray tracing simulations (discussed later) show that these are direct ray multiple paths. Additional support for our conclusion is provided by the wave normal analysis and the electric field measurements described below.

3.2. *Electric Field*

The dots in Figures 4*a* and 4 b give the peak intensities in the fading pattern. These were obtained from electric field charts like those shown in the second and the fourth panel in Figure 3. The average field is a few microvolts per meter, which is consistent with other measurements [*Bell et al.*, 1981, 1983]. The gross behavior of the electric field agrees reasonably with simple estimates from geometric theory. The interesting feature relevant to our present discussion is that the peak intensities of adjacent pulses (separated by a few seconds or equivalently 20 to 30 km in space) differ by 2 to 10 dB, the average fluctuation being around 5 to 6 dB. We attribute this feature to the existence of multiple paths and suggest that at different places multipath signals add in different phases to give the observed intensity fluctuation. Our interpretation discussed in the next section accounts for this feature of the direct ray nonducted multiple paths.

4. INTERPRETATION

We propose a simple mechanism that can be supported on physical grounds and that provides an explanation for the properties of direct ray multiple paths. We postulate the presence of field aligned irregularities of 1 to 10-km horizontal scale with a few percent enhancement or depression in density almost everywhere in the ionosphere. Ionospheric irregularities of much higher magnitude have been observed by *Kelley et al.*[1980] and other ionospheric workers [*Vickrey et al.*, 1980; *Fajer et al.* 1980]. For our interpretation we need irregularities with modest enhancement or depletion in the electron densities. The physical mechanisms of the generation of ionospheric irregularities have been considered by *Vickrey* and *Kelley* [1980].

We explain our proposed mechanism with the help of Figure 5. The ionosphere is assumed to start near 90 km. The boundary between the ionosphere and the magnetosphere is set somewhat arbitrarily at 500 km. Our conclusions do not depend critically on exactly where this boundary is, since the transition from the ionosphere to the magnetosphere is smooth. A typical ISEE 1 satellite trajectory in the magnetosphere is shown at 25000 km altitude.

First consider a smooth, horizontally stratified ionosphere with no irregularities. A VLF pulse at 4 to 5 kHz radiated from a ground source (e.g., Siple transmitter) enters the ionosphere almost vertically, owing to the large refractive index of the ionosphere. As confirmed by ray tracing, the rays starting with vertical wave normals from different latitudes at ionospheric heights reach the high altitude magnetosphere without intersecting each other (This may not be true for waves injected at higher latitudes near the magnetic pole or at higher frequency). This is single direct path propagation.

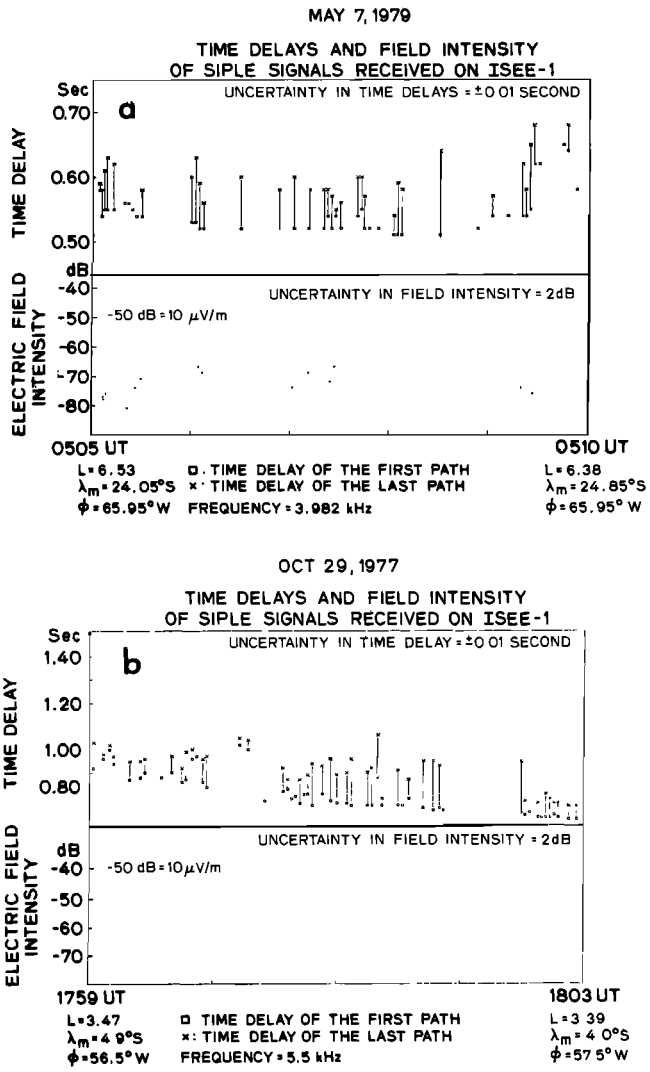

Fig 4. Details of the time delay and field intesity measurements are shown (*a*)for a 5 min period (path length $\approx$ 1500 km) for May 7, 1979 , and (*b*)for a 4-min period (path length $\approx$ 1200 km) for October 29, 1977, respectively. Time delays of the first and the last path are defined as the time delays of the leading and the trailing edge of a transmitted pulse. Pulse elongation is the difference between these two time delays.

Now we introduce small irregularities in the ionosphere, consisting of patches of a few percent of enhanced or depleted ionization of 1 to 10 km horizontal scale. These irregularities generally tend to be field aligned [*Kelley et al.*,1980; *Vickrey et al.*,1980]. For the mechanism presented here the irregularities need not be field aligned. Now a VLF pulse radiated from a ground source enters the ionosphere (at 90 km) almost vertically at all latitudes. Rays starting vertically at different latitudes undergo different amounts of bending depending on the irregularities they pass through and arrive at a height of 500 km with varying wave normals. A simple application of Snell's Law, or ray tracing simulations for an irregular ionosphere, tells us that 1 to 10 km scale size irregularities with a few percent enhanced or depressed ionization lead to 5° to 10° spread in the wave normal direction at 500 km height. The exact distribution of the wave normals depends on the irregularities present in the ionosphere at that time. The important point is that at each latitude at 500 km we no longer have parallel (vertical) wave normals, but rather an angular spectum of wave normals 5° to 10° wide, the nature of which may vary with latitude. At any given latitude, the angular spectum will show intensity peaks in certain directions depending on the irregularities through which the rays have passed. Now as shown in Figure 5, the satellite at any point on its trajectory can receive rays coming from two or more directions. The pulse elongation at a given point will depend on the path difference (in terms of group time delays) between the first and the last rays. This difference in turn depends on the ionospheric locations at which (at 500 km) the injected rays have just the right wave normal angles to reach the satellite. These locations in turn depend on the morphology of the irregularities in the ionosphere at that time. This explains the rather erratic behavior of the pulse elongations.

Figure 6 gives the results of ray tracing simulations. We have assumed that at all latitudes at 500 km we have a 4° spread in the wave normal angles due to the ionospheric irregularities. For the purpose of illustration rays are injected at 58° and 60.2° latitude at 500 km altitude. Now as shown in Figure 6, at point A (B) the satellite can receive two rays: one starting from 58° (60.2°) latitude with 0° initial wave normal angle with respect to the magnetic field, and one starting from 60.2° (58°) latitude with 4° (−4°) initial wave normal angle. The numbers at the top of the trajectory show

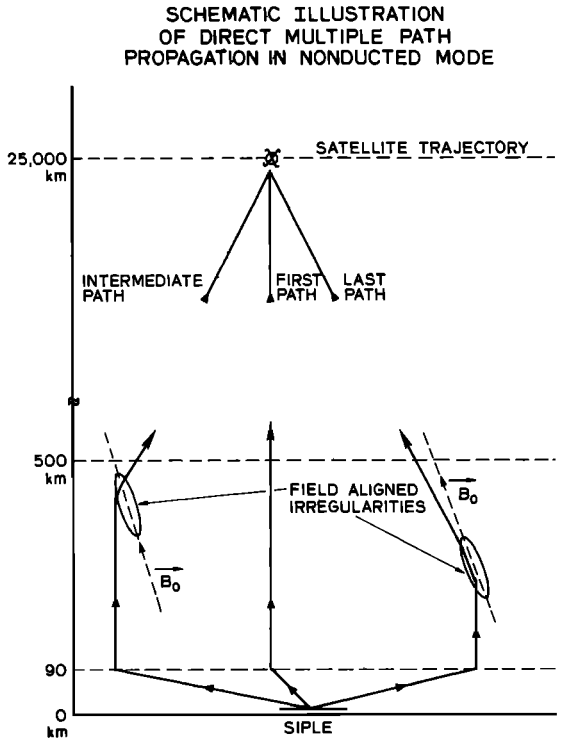

Fig 5. Schematic representation of a mechanism that explains observed direct multipath. We postulate the existence of field aligned irregularities of 1 to 10 km horiontal scale and a few percent enhancement or depletion in the ionosphere. These irregularities can bend the wave normals of the rays starting at the different latitudes at the lower edge of the ionosphere in such a way that more than one ray path reaches the satellite. Time delays of the closely spaced paths are comparable. The bending of the rays shown in the figure is highly exaggerated. In general, 5° of wave normal bending is enough to explain the observed multipath.

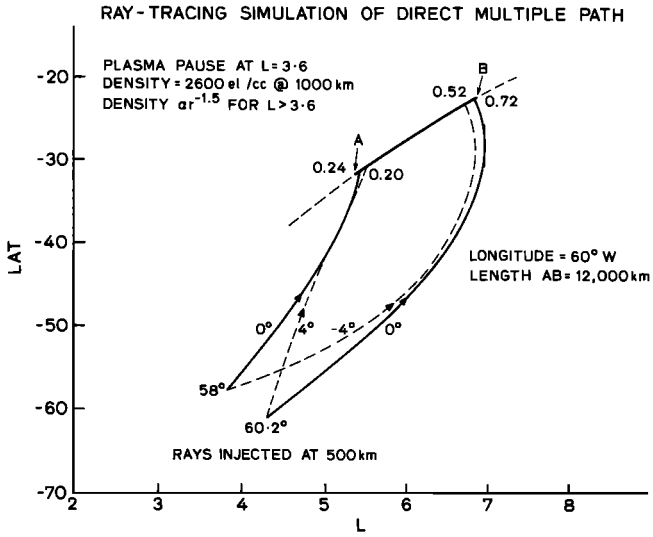

Fig 6. A ray tracing simulation to illustrate direct multiple paths. Rays are injected at 500-km altitude at 58° and 60.2° magnetic latitude. At point A (B) the satellite can receive two rays, one starting from 58° (60.2°) latitude with 0° initial wave normal angle with respect to vertical and one starting from 60.2° (58°) latitude with 4° (−4°) initial wave normal angle with respect to vertical. The numbers at the end of the trajectory show the respective time delays. Notice: (1) Difference in time delays for two rays reaching the same point on the satellite trajectory. (2) A 4° spread in the initial wave normal angle at the ionospheric heights can swing the ray from one end of the 12,000-km long satellite trajectory to the other end.

the respective time delays in seconds. The difference in the wave normal angles of the rays reaching the same point is 5° to 6°. We would like to emphasise a few points regarding the mechanism of direct multiple path propagation.

1. A ray starting at 500 km at any latitude between 58° and 60.2° with appropriate initial wave normal angle between +4° to −4° can reach any point between A and B of the satellite trajectory. Rays which start beyond this latitude range can also reach the satellite trajectory between A and B if they start with initial wave normals higher than 4°.

2. The difference in time delays of two rays reaching the same point A or B is of the same order of magnitude as the measured pulse extensions, supporting the idea that it is the direct multiple path that we observe.

3. In general, a few degrees spread in the initial wave normal angles at ionospheric heights (500 km) can swing the ray thousands of kilometers along a satellite trajectory in the magnetosphere.

Thus a simple assumption about the existence of small irregularities in the ionosphere leads to an explanation of the observed features of the multiple path propagation, including its common occurence.

5. Wave Normal Analysis

In this section we introduce a new method to analyze the wave normal information contained in the electric field measured by a spining antenna. The results quoted here provide additional support for the interpretation of the previous section. The details of this new technique are the subject of a future paper[*Sonwalkar et al.*, 1984].

The ISEE 1 satellite and therefore the receiving antenna, spins at a fixed angular speed of 3.04 s/revolution. The spin axis is generally pointed within 1° of the perpendicular to the ecliptic plane, causing fading of the received signal. In general, the fading period will be half the spin period if the wave normal is limited to one single direction. The fading pattern gives two experimentally measured parameters, viz. the depth of fading and the phase of fading (i.e., when the maxima or minima occur in the fading pattern with respect to the known angular position of the antenna in the spin plane). Therefore, if we assumed whistler mode wave propagation, and if the plasma density is known, it becomes possible to estimate the wave normal direction (the polar as well as the azimuthal angles) from the measured parameters. Very often the wave satisfies the condition for quasi-longitudinal propagation[*Helliwell*, 1965]. In this case one need not know the cold plasma density. In the case of multiple paths, waves coming from different directions introduce different doppler shifts in the frequencies observed as a result of the $\approx$ 5 km/s satellite motion. This results in additional fading periods (or frequencies). Since the doppler shift is a function of the wave normal direction as well as the magnitude, and because the latter depends on the local plasma density , we need to know the cold plasma density in the case of multiple wave normals. We have used the measured geomagnetic field in our calculations, whenever such data were available. Otherwise, a dipole model is assumed. A full analytical theory to deduce a single wave normal as well as multiple wave normal directions from the observed fading pattern has been developed. A computer code was written to extract a single wave normal or the dominant wave normal in the presence of weak multiple paths. We give the result of the simple case when there are only two wave normals (or equivalently two ray paths) present. The crux of the analysis lies in the slowly varying envelope approximation, which assumes that the amplitude remains constant over many cycles of the wave frequency. The justification for this assumption comes from the observed fading patterns. In the case of two wave normals, the amplitude envelope is given by

$$\begin{aligned} v_e = [&A + B\cos(2\omega_s t + \phi_B) \\ &+ C\cos(\Delta_\omega t + \phi_C) \\ &+ D\cos((2\omega_s - \Delta_\omega)t + \phi_D) \\ &+ E\cos((2\omega_s + \Delta_\omega)t + \phi_E)]^{1/2} \end{aligned} \quad (1)$$

Where A, the dc amplitude, the constants B, C, D, and E, and the phase factors ϕ_B,ϕ_C,ϕ_D, and ϕ_E are functions of the two wave normals ($\mathbf{k}_1$ and $\mathbf{k}_2$) and the relative strengths ($\mathbf{E}_1$ and $\mathbf{E}_2$) of two signals coming from two different directions, $2\omega_s$ is twice the angular frequency of the antenna spin and Δ_ω is the differential doppler shift between the two wave normal components as observed by the satellite. The bottom panel in Figure 3 is an example of two discrete multiple paths. A fourier transform of the amplitude envelope shown here gives five discrete frequncy components (including one at dc) as predicted by equation (1). Doppler shift measurements are generally difficult because the noise introduced due to tape flutter is of the same order of frequency as the doppler shifts. However, the tape flutter is eliminated in the envelope of the received voltage making it possible to make differential doppler measurement. It is the measured differential doppler that contains the multipath information.

Detailed analysis of these kind of signals is presented in a separate paper[*Sonwalkar et al.,* 1984].

For the case of only one wave normal we get

$$v_e = \sqrt{A(\mathbf{k},\mathbf{E}) + B(\mathbf{k},\mathbf{E})\cos(2\omega_s t + \phi_B)} \qquad (2)$$

Where A, B, and ϕ_B are related to the wave normal direction.

From equations (1) and (2) we see that the fading pattern is the square root of a simple sinusoid for a single wave normal and becomes more complicated as an additional path is introduced. More time periods are introduced in the fading pattern in the presence of more paths. Complicated patterns as predicted by a more generalized form of equation (1) for three or more ray paths appear in nearly every case of Siple signals observed on ISEE 1 satellite. This provides additional support for our conclusion regarding the common occurrence of multiple paths. For example on May 7, 1979, two dominant wave normal directions were observed, one at 25° and one at 40° with respect to the geomagnetic field. On October 29, 1977, a dominant wave normal was observed at about 50° angle with respect to the geomagnetic field. These calculations were also confirmed by the ray tracing simulations for the respective days. The details of wave normal measurements and their use in plasma diagnostics will appear in a future paper.

Estimation of the wave normal vector in space has been a difficult problem and therefore point by point wave normal measurements in space have not been performed in the past [*Shawhan,* 1983]. Previous work has employed 3 to 6 components of measured electric and magnetic field to extract the wave normal information in the cases of a single plane wave, a combination of plane waves, or a general wave distibution function [*Leufeuvre et al.,* 1982; *Storey and Lefeuvre,* 1974; *Shawhan,* 1970,1983]. In a recent paper by *Lefeuvre et al.* [1982], wave normal directions and wave distribution functions were determined for seven Omega transmitter pulses observed on the GEOS 1 satellite. They find, in general, a single peaked distribution of the wave normals for each pulse. They also find a 0.2 to 0.4-s periodicity in the wave normal directions, which is interpreted in our technique as two closely spaced multipath. They find that, for low signal to noise ratio, signals behave like a random process and give a wide wave distibution function, and for high signal to noise ratio signals behave like a deterministic process and give a narrower wave distribution function. The new method of wave normal analysis developed here differs from those in the past, in that it provides a quick method to detect the presence of multiple path from just the visual inspection of the observed fading pattern. It can also compute the dominant wave normal direction in a very simple way. However, our method assumes that the wave structure is a combination of plane waves that remains constant over a few seconds of the satellite trajectory and that these waves obey the whistler mode dispersion relation. In that sense it is less general than Lefeuvre's method. In the case of ISEE 1 satellite observation of Siple signals the observed fading patterns justify our assumptions.

6. CONCLUSION AND IMPLICATION

1. We conclude that within the domain of our measurements (L=2.8 to L=11.5, latitude range from 40° south to 60° north, longitude range from 40° west to 140° west) a signal transmitted from the ground arrives almost simultaneously at a satellite (within 100 to 200 ms) along two or more direct ray paths. We expect this result to hold in other parts of the magnetosphere as well. Our results are important for radio diagnostics of the magnetosphere and wave particle interaction studies because a kind of "randomness" is introduced in the wave stucture (of a wave injected from the ground) at magnetospheric locations owing to small irregularities in the ionosphere. In an analogous manner we can infer that the wave normal directions of nonducted waves trapped in the magnetosphere will smear out as the waves bounce back and forth between the two hemispheres.

2. The existence of multiple paths has important implications for nonducted wave-particle interactions. Here we shall briefly mention two consequences of our results. (1) From a preliminary study it appears nonducted waves can be approximated as combinations of simple plane waves over a distance less than 100 km. (2) The spread in the wave normal directions due to multiple paths reaching a point in the magnetosphere leads to a doppler broadened signal for an electron moving along a field line. The width of the doppler spectrum Δf for a gyroresonant particle is given by

$$\Delta f = \frac{(f_H - f)(1 - \frac{Y}{2}\cos\theta)}{Y\cos\theta - 1}\sin\theta\Delta\theta \qquad (3)$$

where $Y = f_H/f$, f_H, and f are the local gyrofrequency and wave frequency, respectively, θ is the wave normal direction with respect to the local geomagnetic field direction, and $\Delta\theta$ is the spread in the wave normal direction due to multiple paths.

For f_H = 10 kHz, f = 5 kHz, Y = 2, and $\Delta\theta$= 5° we obtain

$$\Delta f = 0\,\text{Hz} \qquad \theta = 0°$$
$$\Delta f = 40\,\text{Hz} \qquad \theta = 30°$$
$$\Delta f = 400\,\text{Hz} \qquad \theta = 50°$$

Components of the multiple path wave structure will interfere over a time scale $\tau \approx \Delta f^{-1}$. This suggests that coherent interaction between the energetic electrons and the nonducted waves may take place over shorter distances than the 1000 to 2000 km hypothesized for the ducted case [*Helliwell,* 1967]. On the other hand a larger number of particles might take part in the interaction due to the increased apparent bandwidth. A detailed wave particle interaction theory along these lines might provide a key to the observed broadband and fast rising nature of VLF emissions triggered by nonducted coherent VLF waves [*Bell et al,* 1981].

3. Because path multiplicity originates in ionospheric irregularities, measurement of the related wave normal angles, pulse elongations , and the electric field fluctuations may lead to a new technique of ionospheric irregularity diagnostics. One can think of the magnetosphere as a medium that acts as an amplifying lens for looking at small irregularities in the ionosphere.

4. From the discussion given above it appears that effects analogous to multiple path propagation should be seen when studying the ionospheres of other planets, interplanetary space, etc., with a radio source on a satellite and a receiver in the far field. As mentioned in conclusion (3), the process could be reversed and the phenomenon can be used to study the structures (or irregularities) in these mediums. Such studies have been carried out in the high-frequency

range [*Tyler et el.*, 1981]. Here we suggest that these techniques can be extended to the VLF range with one difference that the receiver should also be in space. One can possibly apply the phenomenon to more practical problems in other areas; for example, the study of miniature faults in materials using acoustic waves etc.

Acknowledgments. This research was supported by the National Aeronautics and Space Administration under grants NGL-05-020-008 and NAS 5-27544.

The editor thanks F. Lefeuvre and E. Ungstrup for their assistance in evaluating this paper.

REFERENCES

Bell, T. F., and R. A. Helliwell, The Stanford University VLF wave injection experiment on the ISEE-1 spacecraft, *IEEE Trans. Geosci. Electron., GE-16,* 248, 1978.

Bell, T. F., U. S. Inan and R. A. Helliwell, Nonducted VLF waves and associated triggered emissions observed on the ISEE-1 satellite, *J. Geophys. Res., 86,* 4649, 1981.

Bell, T. F., R. A. Helliwell, U. S. Inan, I. Kimura, H. Matsumoto, T. Mukai, and K. Hashimoto, EXOS-B/Siple station VLF wave-particle interaction experiments,2, transmitter signals and associated emissions, *J. Geophys. Res., 88,* 295, 1983.

Cerisier J. C., A theoretical and experimental study of non-ducted VLF waves after propagation through the magnetosphere, *J. Atmos. Terr. Phys., 35,* 77, 1973.

Chang, D. C. D., VLF wave-wave interaction experiments in the magnetosphere, *Tech. Rep. 3458-1,* Stanford Electron. Lab., Stanford, Calif., 1978.

Edgar, B. C., The stucture of the magnetosphere as deduced from magnetospherically reflected whistlers, *Tech. Rep. 3438-2,* Stanford Electron. Lab., Stanford , Calif., 1973.

Fejer, B. G., and M. C. Kelly, Ionospheric irregularities, *Rev. Geophys. Space Phys., 18,* 401, 1980.

Helliwell, R. A., *Whistlers and Related Ionospheric Phenomena,* Stanford University Press, Stanford, Calif., 1965.

Helliwell, R. A., A theory of discrete VLF emissions from the magnetosphere, *J. Geophys. Res., 72,*4773, 1967.

Heyborne, R. L., Observations of whistler-mode signals in the OGO satellites from VLF ground station transmitters. *Tech. Rep. No. 3415/3418-1,* Stanford Electron. Lab., Stanford, Calif. 1966.

Kelley, M. C., K. D. Baker, J. C. Ulwick, C. L. Rino, and M. J. Baron, Simultaneous rocket probe, scintillation, and incoherent scatter observations of irregularities in the auroral zone ionosphere, *Radio Sci.,15,* 491, 1980.

Lefeuvre, F., T. Neubert, and M. Parrot, Wave normal directions and wave distribution functions for ground-based transmitter signals,*J. Geophys. Res., 87,* 6203, 1982.

Neubert, T., E. Ungstrup, and A. Bahnsen, Observations on the GEOS 1 satellite of whistler mode signals transmitted by the omega navigation system transmitter in northen Norway, *J. Geophys. Res., 88,* 4015, 1983.

Scarabucci, R. R., Interpretation of VLF signals observed on the OGO-4 satellite, *Tech. Rep.3418-2,* Stanford Electron. Lab., Stanford, Calif. 1969.

Shawhan, S. D., The use of multiple receivers to measure the wave charecteristics of very-low frequency noise in space, *Space Sci. Rev., 10,* 689, 1970.

Shawhan, S. D., Estimation of wave vector characteristics, *Adv. Space Res., 2,* 31, 1983.

Smith, R. L., R. A. Helliwell, and I. Yabroff, A theory of trapping of whistlers in field-aligned columns of enhanced ionization. *J. Geophy. Res., 65,* 815, 1960.

Sonwalkar, V. S., T. F. Bell, R. A. Helliwell, and U. S. Inan, Direct multiple path magnetospheric propagation: A fundamental property of the VLF non-ducted waves transmitted from Siple Station, Antartica, paper presented at AGU Fall Meeting, San Francisco, December 7-15, 1982.

Sonwalkar, V. S., T. F. Bell, R. A. Helliwell, and U. S. Inan, An analysis of electromagnetic signals received by a single spinning antenna aboard a satellite, to be submitted to *Radiosci.,* 1984.

Storey, L. R. O., and F. Lefeurve, Theory for the interpretation of measurements of a random electromagnetic field in space, *Space Res.,15,* 381, 1974.

Tyler, G. L., V. R. Eshleman, J. D. Anderson, G. S. Levy, G. F. Lindal, G. E. Wood, and T. A. Croft, Radioscience investigations of the saturn system with voyager 1: Preliminary results, *Science, 212,* 201, 1981.

Vickrey J. F., C. L. Rino, and T. A. Potemra , Chatanika/Triad observations of unstable ionization enhancement in the auororal *F* region, *Geophys. Res. Lett. , 7,* 789, 1980.

Walter, F., Nonducted VLF propagation in the magnetosphere. *Tech. Rep., SEL-69-061,* Radiosci. Lab., Stanford Electron. Lab., Stanford, Calif., 1969.

T. F. Bell, R. A. Helliwell, U. S. Inan, and V. S. Sonwalkar, Space, Telecommunications and Radioscience Laboratory, Stanford University, Stanford, CA 94305.

(Received September 2, 1983;
revised January 23, 1984;
accepted January 25, 1984.)